Layered Composite Model for Design and Fabrication of Bone Replacement

B. Starly, J. Nam, W. Lau, W. Sun[*]

Department of Mechanical Engineering and Mechanics
Drexel University
Philadelphia, PA-19104

Abstract

Biological tissues are inherently heterogeneous. The design of 3D tissue scaffolds for tissue engineering application should, if possible, biomimic the complex hierarchy and structural heterogeneity of the replaced tissues. This is particularly true for design of bone scaffolds with structural properties compatible with the spatial heterogeneity and mechanical properties of the replaced tissue. The paper presents an image-based computer modeling approach for reconstruction, characterization, and biomimetic modeling and design of three-dimensional heterogeneous tissue structure. The presented work will cover: 1) overview of biomimetic modeling and design of bone structures and reverse engineering for CAD-based constructive solid geometry; 2) design of bone scaffold; and 3) slicing and process planning for solid freeform fabrication.

1. Introduction

The need for organ and tissue substitutes to repair or replace damaged or diseased organs or tissues is on an increasing demand in the United States [1-3]. Bone substitutes are often required to help repair or replace damaged or diseased tissues in cases ranging from trauma, to congenital and degenerative diseases, to cancer, and to cosmetic needs. Currently available bone substitutes, including auto grafts, allograft, and synthetic materials, are the most implanted materials in surgeries conducted countrywide. However, these substitutes are far from ideal and have many associated problems, e.g., auto-grafts are expensive and can have significant donor site morbidity, and synthetic materials wear and do not behave like natural bone. The need for bone substitutes is particularly important in such a scenario. New advances in scaffold guided tissue engineering [4-7] may provide solutions to overcome the limitations.

Generation of functional tissue or organ structure requires a scaffold to guide the overall shape and three-dimensional organization of multiple cell types. The internal architecture of a bone scaffold cannot be chosen at ease and various factors need to be considered, such as porosity, pore size, and interconnectivity of the tissue scaffold structure have all been identified to be important factors that make a tissue scaffold successful [8-10]. These factors aid in transportation of nutrients that would enable the further growth of new cells and allow the tissue scaffold to act as a suitable template for appropriate bone ingrowth and healing. In addition, the designed scaffold structure should be able to have required mechanical strength after implantation, particularly in the reconstruction of hard and load bearing tissues such as bone and cartilage. The strength of biodegradable tissue scaffolds must not decline rapidly and must degrade at a rate similar to the growth of new tissue cells. Therefore tissue scaffold structure

---

[*] Corresponding author

should be compliant both biologically as well as mechanically at the site of implantation and should at best mimic the natural bone properties in order to function as a true bone substitute.

The objective of this paper is to present a biomimetic modeling approach for design and fabrication of a bone tissue scaffold structure. Section 2 presents an overview of our approach to model a heterogeneous bone structure as well as various process paths to arrive at a CAD-based bone heterogeneous model reconstructed from non-invasive medical images; Design and characterization of different scaffold unit cells is presented in Section 3; followed by a fabrication planning solid free form fabrication in Section 4, and a summary, discussion and conclusions in the last section.

2. A CAD-based Biomimetic modeling and design of heterogeneous bone structure

Bone tissue scaffolds need to have certain characteristics of their own in order to function as a true bone substitute that satisfy the biological, mechanical and geometrical constraints [1]. Such characteristics include: 1) Biological requirement -- The designed scaffold must facilitate cell attachment and distribution, growth of regenerative tissue and facilitate the transports of nutrients and signals. This requirement can be achieved by controlling the porosity of the structure, by providing appropriate interconnectivity inside the structure, and by selecting appropriate biocompatible materials. 2) Mechanical requirement -- The designed scaffold must provide structural support at the site of replacement while the tissue regenerates to occupy the space defined by the scaffold structure. Scaffold structures need to be defined to possess the required mechanical stiffness and strength of the replaced structure; and 3) Anatomical requirement -- It must be of an appropriate geometric size that fits in at the site of replacement.
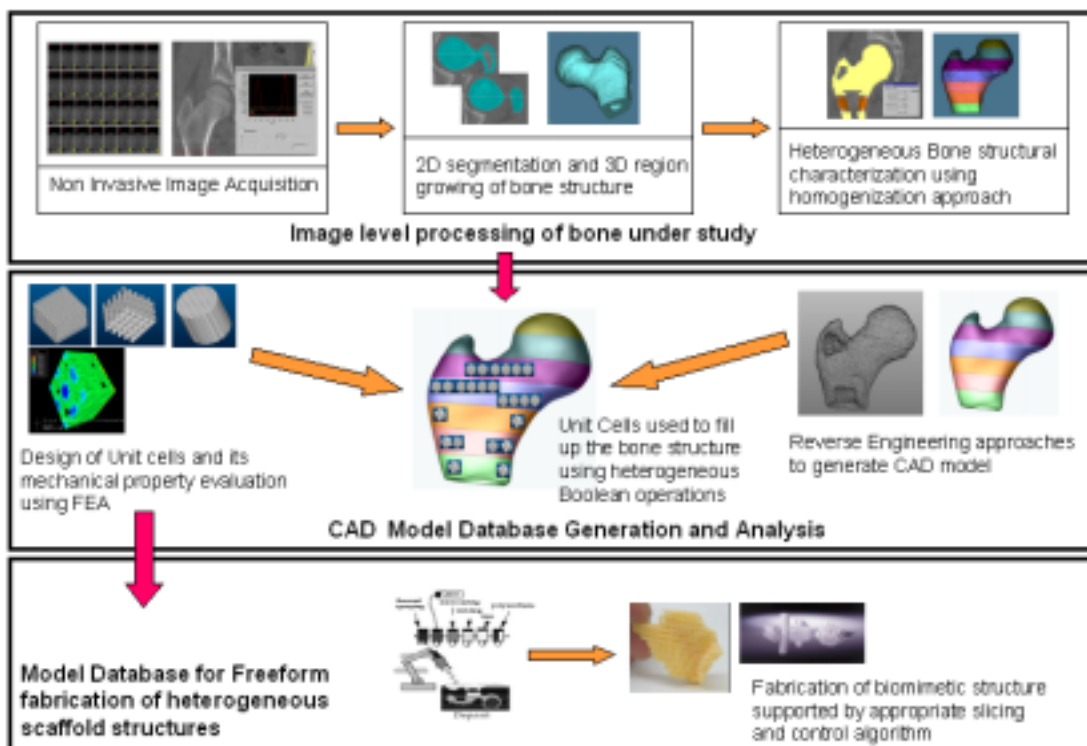

Figure 1: Overview of biomimetic modeling and design of bone scaffold

25

We have recently developed a biomimetic modeling approach for design of tissue scaffolds, prostheses and implant, and for tissue identification [11-13]. This approach adopts the enabling technological developments in computer-aided design, in medical image processing, and in solid freeform fabrication and address above design considerations into the tissue scaffold design, for example, designing scaffolds with specific internal architecture, porosity, pore interconnectivity, and selected biomaterials and specified geometry. Figure 1 illustrates an overview of the biomimetic modeling and design approach. A brief procedure is presented as follows.

Our design approach begins with the acquisition of noninvasive image and its subsequent processing of appropriate bone region of interest. This is followed by a three-dimensional reconstruction of anatomical structure using commercially available medical reconstructive and reverse engineering software (MIMICS [14] and Geomagic [15]). The next step is to appropriately devise a process by which tissue structural heterogeneity can be characterized through a homogenization technique. Candidate unit cells to make up the bone scaffold would be designed using CAD software (Pro/Engineer [16]) and analyzed for its mechanical properties using finite element method. Appropriate unit cells would be then integrated with the shape of the bone to form the bone tissue scaffold with specified internal architecture and structural properties to match that of the actual bone based on the characterization analysis.

Step 1: Image Acquisition.

Our region of study involved the CT images obtained from that of a proximal femur bone of a small child. In all, 34 sliced images were obtained each of 2mm slices thereby totaling a length of 68mm of the proximal femur bone. These sliced images were loaded into MIMICS and organized in a sequential manner and oriented for its top, bottom, anterior, and posterior positions.

Step 2: Segmentation and Characterization Process

Once loaded, the region of interest was identified and a 3D voxel model of the bone under study had to be made. As a first step, an appropriate threshold range was found that could best capture the relevant information contained in the femur. Using this threshold value, all pixels within this range were grown to a color mask and hence the segmentation process achieved by making use of region growing techniques available in the software. The segmentation was achieved using two different approaches, each approach serving a particular purpose. In the first approach, the whole proximal femur structure was grown into one single color mask representing one single threshold range. With this approach, the average threshold value for the whole structure could be obtained. This average threshold value was in turn correlated to the QCT# represented in Hounsfield units (HU) by using a simple relation as follows:

$$QCT\# = \text{Threshold Value} - 1024 \qquad\qquad (1)$$

In the second approach which is the homogenization technique, the femur structure was divided into layers and then an average QCT# for each layer found. A collection of slices of the femur was grouped as layers and segmented using different color masks. Each layer thickness was about 10mm and around 7 layers in all. An average QCT number was obtained for each layer in order to characterize the tissue heterogeneity (Fig 2). The QCT number retrieved from the appropriate layers is then correlated to the density of the bone by a linear interpolation using relations available in published papers. This density can in turn be then related to E, allowing the heterogeneous elasticity of the bone to be defined [17, 18]

For QCT < 816: $\rho = 1.9 \times 10^{-3} * QCT + 0.105$ and $E = 0.06 + 0.9 * \rho^2$ (2)
For QCT > 816: $\rho = 7.69 \times 10^{-4} + 1.028$ and $E = 0.09 * \rho^{7.4}$ (3)

The structural heterogeneity of the bone can thus be defined through the associated bone Young's modulus. The characterization results are shown in the table in Figure 1. The last row in the table indicates the QCT# retrieved when a single color mask was considered.
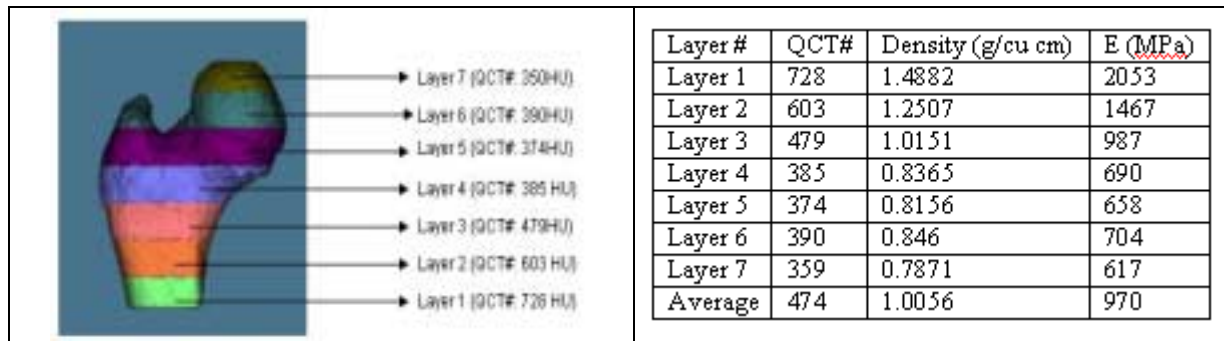

Layer #	QCT#	Density (g/cu cm)	E (MPa)
Layer 1	728	1.4882	2053
Layer 2	603	1.2507	1467
Layer 3	479	1.0151	987
Layer 4	385	0.8365	690
Layer 5	374	0.8156	658
Layer 6	390	0.846	704
Layer 7	359	0.7871	617
Average	474	1.0056	970

Figure 2: Layered heterogeneous model determined by QCT characterization

Step 3: CAD model generation

Once the bone heterogeneity has been characterized, a complete CAD-based structure model of the anatomical geometry needs to be defined. A reverse engineering approach that converts 3D reconstructive image data to a NURBS-based CAD model will be developed. We have evaluated and compared three different process paths for generating a CAD model from MRI/CT data as shown in Fig. 3. The comparison and comments of these three paths are also listed in Table 1.

Process Path 1: MedCAD interface

This interface bridges the gap between medical imaging and CAD design software. This means that this interface can export data from the imaging system to the CAD system and vice versa. The IGES format is used for models to be exported to CAD and the STL format used to import models from CAD to the MedCAD system. Basic features can be recognized and converted to geometrical entities such as cylinder, sphere, anatomical landmarks etc. B-Spline surfaces are also used to make a real fit on a surface anatomical contour. It is important to realize that not all features or details of the image can be exported to CAD due to the limitation of this interface, particularly for features with complex geometry.
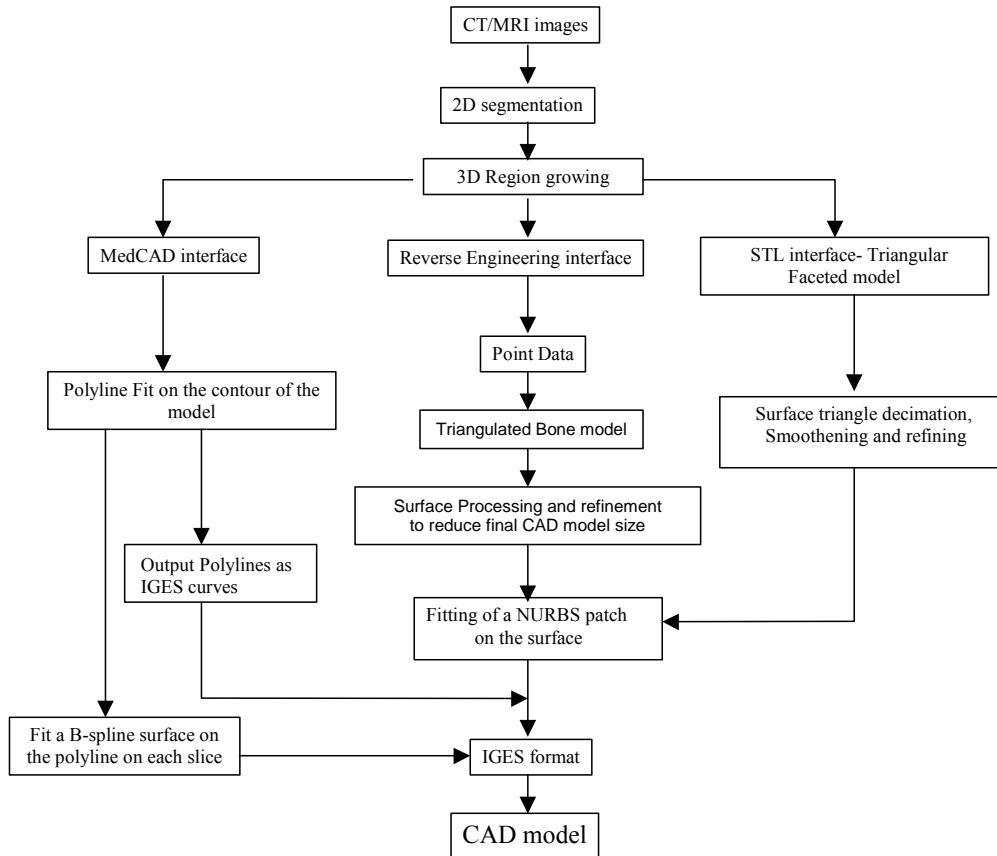
27

Figure 3: Three different process paths for generating a CAD model from MRI/CT data

Table 1: Comparison of different paths for the proximal femur

Process	Comments	Model sizes	Quality
MEDCAD Interface	Easiest and quickest, but may not be suitable for complex models.	Does not involve huge file sizes and only involves the IGES conversion process time. IGES: 266KB CAD (Pro-E): 309KB	Poor
Reverse Engineering Method	A longer process but suitable for complex shapes since control is achieved at every level.	Initial file sizes in the point form are not high but final CAD model may involve comparatively high file sizes. Point: 256KB (around 7732points) IGES: 266KB (102 NURBS patches) CAD (Pro-E): 298KB	Best
STL Interface	Quicker method to arrive at a CAD Model but may not work for complex surfaces	Initial STL file size maybe high resulting in more CAD model IGES file size. STL: 1.82 MB (38252 triangles) IGES: 9.83MB (2316 NURBS patches) CAD (Pro-E): 10.3MB	Average

Process Path 2: Reverse Engineering Method

The 3D voxel model created after segmentation is used as the starting point for this method. The 3D voxel dataset of the bone structure is converted to point data form and then these points are loaded into any reverse engineering software. Commercially available software

Geomagic Studios (Raindrop Inc) was then used to process these data points for surface processing and refinement. This is perhaps the best approach that can be followed since the process starts from the base level, i.e., points. Although the model could have a comparatively longer processing time, the results obtained are significantly better than the other two methods.

Process Path 3: The STL interface.

The 3D voxel model can also be converted to the STL file and this STL file can then be imported into Geomagics for surface refinement and NURBS surface generation. The difference between this and the point data method is that here a triangulated model is the input format rather than the point data form of the structure. The process time involved is less but maybe suitable for only certain kinds of surfaces.

The final CAD model of the proximal femur structure obtained by each of the process path is shown in Figure 4. Notice that the femur structure obtained by the STL process path has resulted in a poor CAD model. The smoother the model, file sizes tend to be lower and can be less frustrating while handling these models in CAD software. The reverse engineering method was followed for the CAD model generation of the homogenized femur domain structure since this resulted in a much smooth and better model and more importantly had a smaller file size of around 12MB (SOLIDWORKS) for all the seven layers combined. The seven-layered CAD assembly structure of the proximal femur is also shown in Figure 4.
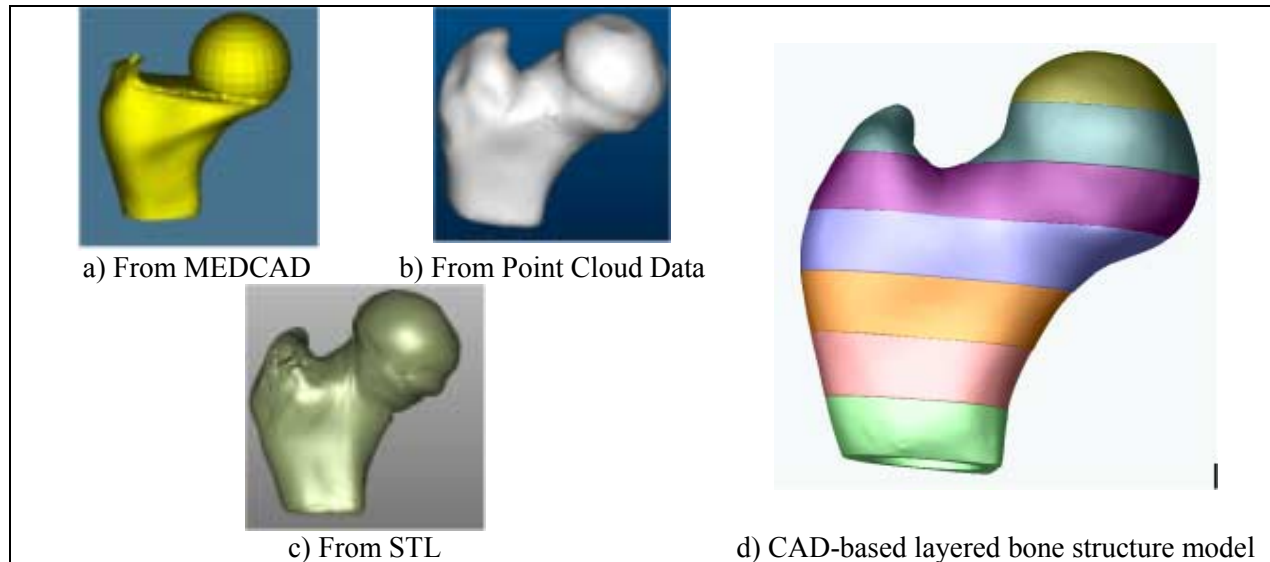

a) From MEDCAD b) From Point Cloud Data

c) From STL d) CAD-based layered bone structure model

Figure 4: CAD based bone structure model

3. Design and characterization of bone scaffold unit cell

Cellular scaffold unit cells with varying porosity and internal architectures can provide tailored mechanical and biological properties. In this work, we use feature primitives in which each primitive discrete volume is represented by a specific design feature, such as different internal architecture patterns used in common tissue scaffold design. We further use the feature patterns and architectures to design desirable pores, pore sizes and shapes, and its distribution in

the scaffold internal structure so the required mechanical and biological conditions can be met. We then select the specific feature primitive as the unit cell internal architecture according to the required mechanical or biological functions, and use the heterogeneous CAD modeling approach to construct unit cells for bone scaffold, in considering the anatomical and topological requirements for bone replacement. Samples of CAD-based cellular unit cell rendered images are shown in Figure 5. A finite element method (ABAQUS) was then used to predict the unit cell effective mechanical properties and results of a basic unit cell are shown in Figure 6 for the unit cell with characteristic geometrical parameters (Fig. 6a), applied boundary condition (Fig. 6b), and the contour plot of the reaction force (Fig. 6c).
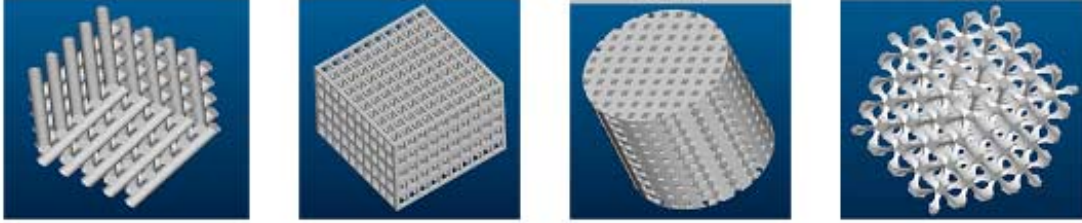

Figure 5: Samples of designed cellular Unit Cells

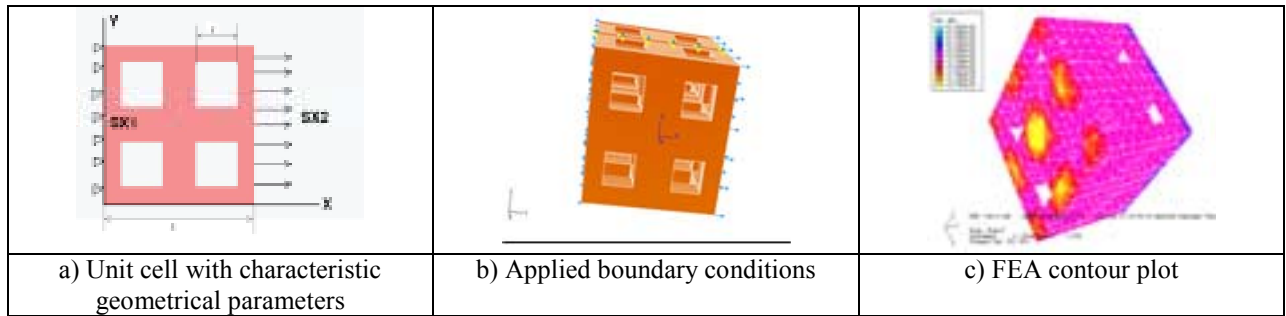| a) Unit cell with characteristic geometrical parameters	b) Applied boundary conditions	c) FEA contour plot

Figure 6: FEA Results of a Basic Unit Cell

The unit geometry is 4.5 x 4.5 x 4.5mm with 4 pore holes on each face. The scaffold cellular unit cell model was generated in Pro/Engineer, and converted to IGES format and then imported to ABAQUS for finite element analysis. A total 8353 4-node tetrahedral elements were used in the analysis. The average reaction force Rx was calculated for every node on the constrained surface (Fig. 6c) and used to calculate the effective modulus E_{xx} based on equation (7). Results of the designed varying sizes of the unit cell to model various porosities vs. different biomaterials of Hydroxyapatite, L-PGA and L-PLA are plotted in Figure 7.

$$E_{XX} = \frac{\sigma_X}{\varepsilon_X} = (\frac{R_X}{A_{SX2}})/(\frac{U_X}{L_X}) = \frac{R_X}{0.001 * A_x} \qquad (4)$$

The relationship of the porosity with the overall geometry of the unit cell for the homogeneous square unit cell with square pores, is determined by:

$$P = \frac{N[\{L * l^2 * (f/2)\} - \{(f/2 - 1) * l^3 * N/2\}]}{L^3} \qquad (5)$$

where N is the number of the pores in the unit cell; f is the total number of faces that contain pores, L is the size of square unit cell and l is the size of pore (Fig. 6a). From the QCT characterization of the proximal femur, the bone Young's modulus varies from 0.6 to 2.0GPA.

From a biological point of view, we know that a desirable scaffold structure should have a porosity ranging from 55-70%. In this regard, the unit cell made of hydroxyapatite material with 59% porosity and effective Young's modulus of 0.6734GPa barely meet both biological and mechanical requirements. L-PLA-based unit cells with around 40 - 60% porosity do give a better option as a scaffold material for the proximal femur. Candidate unit cells can then be selected from the predicted curves shown in Figure 7.
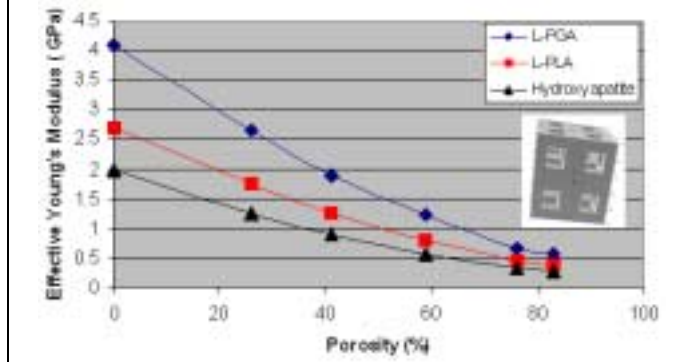

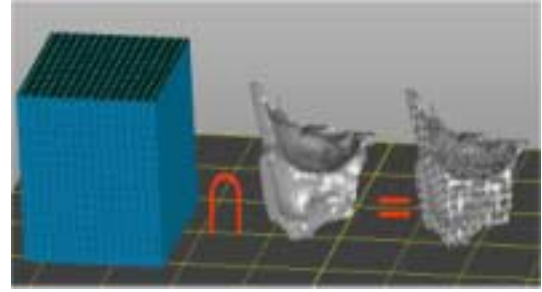| Fig. 7: Effect of unit cell material and porosity on unit cell mechanical properties	Fig. 8: Example of using Boolean operation to achieve the bone anatomical structure

Once the appropriate unit cell has been identified with the matched porosity, interconnectivity, and mechanical properties, a contour bone structure reconstructed from CT/MRI images will be filled in with the selected unit cell architecture. A constructive heterogeneous solid geometry algebra [19, 20] can be used to combine the unit cell architecture and the replaced bone anatomical structure to achieve the final shape of the replaced bone tissue scaffold. Example of how a basic unit cell was intersected within Geomagics software with a bone structure that needs to be replaced to form a tissue scaffold of the exact internal architecture and external anatomy is schematically illustrated in Figure 8.

We can also consider the structural heterogeneity of bone as an n-layered laminated composite. This model is analogous to real bone replacement/scaffold structure produced through layered solid freeform fabrication technology (for example, stereo lithography-SLA, laminated objective manufacturing-LOM, and three-dimensional prirnting-3DP). The overall effective mechanical properties of bone structure are anisotropic and can be determined through a composite lamination theory. At the laminar level, a unit cell is used to calculate the laminar effective properties. The average linear stress-strain relations of the unit cell in the k_{th} layer in this model can be expressed by

$$\overline{\sigma}_{i,j} = \overline{C}_{ijpq}\overline{\varepsilon}_{qp} \tag{6}$$

where

$$\overline{C}_{ij} = \sum_{k=1}^{n}\alpha^{k}[C_{ij}^{(k)} - \frac{C_{i3}^{(k)}}{C_{33}^{(k)}}] + \sum_{k=1}^{n}\alpha^{(k)}\frac{C_{13}^{(k)}}{C_{33}^{(k)}}\sum_{l=1}^{n}\alpha^{(l)}\frac{C_{3j}^{(l)}}{C_{33}^{(l)}}(\sum\frac{\alpha^{(k)}}{C_{33}^{(k)}})^{-1} \quad (\text{ i =1,2,3…}) \tag{7}$$

represents the average effective elastic tensor of the bone; C_{ij} the elastic components of the kth layer and $\alpha^{k}=h_{k}/h$, with h denoting the total height of the bone and h_{k} the height of each layer.

4. Proposed process planning for layered fabrication of bone replacement

A sample process-planning scenario to design and fabricate tissue scaffold structures is depicted in Figure 9. In the custom implant planning stage, the CT/MRI images of the defected region are obtained and reconstructed by the method as we have already outlined in the previous section. Through reverse engineering techniques, a CAD model of the region of interest is made. At the same time, mechanical characterization techniques would be employed to obtain the mechanical properties of the region to be replaced. Based on the characterization process and biological requirements, an appropriate unit cell designed and along with constructive heterogeneous solid geometry techniques an appropriate scaffold structure obtained. The CAD file is then converted to the STEP (Standard for Exchange of Product model data) file format. [21, 22] has the ability to transfer exact geometry information together with information such as material properties, surface finish and tolerances, and support to heterogeneous objects [23-25]. The STEP file is then imported into a fabrication planning software. Using an appropriate 3D kernel, the scaffold implant reconstructed from the STEP definitions and then appropriately sliced depending on the slice parameters set using the slice module of the software. The slice module based on the direct slicing approach would directly work on the B-rep structure in the STEP file. Due to the direct slicing method, geometrical accuracy is maintained removing the inefficiencies of the STL format.
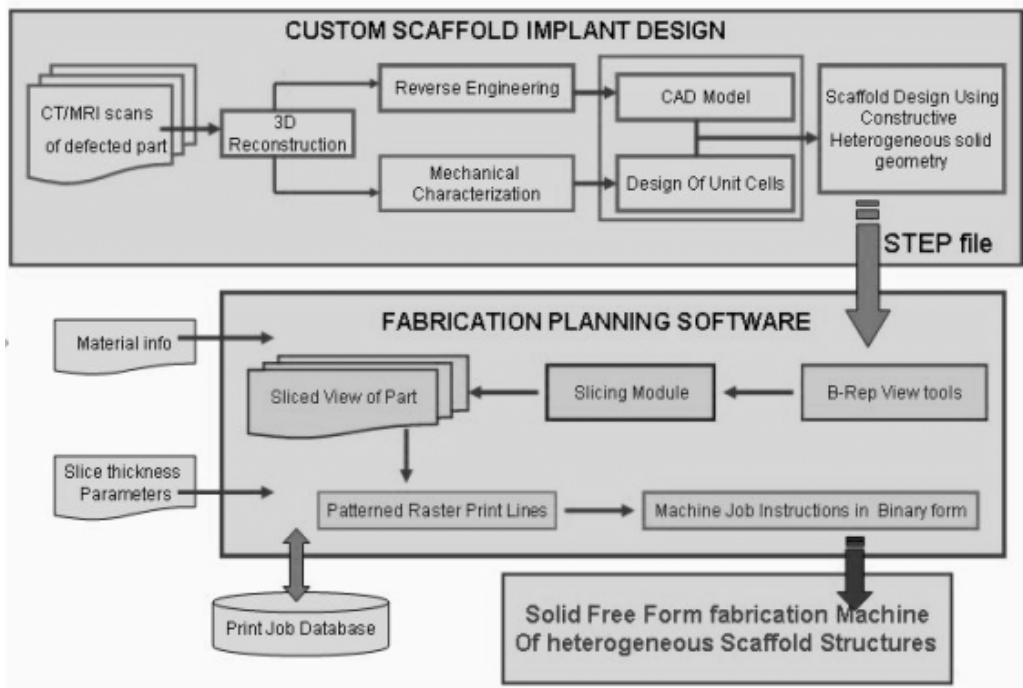

Figure 9: Proposed process plan to fabricate a bone tissue scaffold

The slicing is achieved based on the ray-casting method where the object is sliced by a series of planes and each planes having rays shoot out across them. The intersection points of the ray with the object define an entry point and exit point. A set of these points define raster lines. The slicing module defines the slice layers as scan raster lines to support the open-end architecture that is required for the scaffold structures. Once these scan lines are defined,

complete information which consists of the slice layers as well as the material information is stored in a print job database that serves as a buffer zone as well as for future retrieval. The scan lines are converted to machine code instructions, which are then sent to the machine for fabrication.

5. Conclusion

This paper presented our recent study on the development of computer modeling approach for characterization and design of a biomimetic 3D heterogeneous bone structure. The modeling approach, QCT characterization method, and a CAD based scaffold bone scaffold design were described. Results of the effect of the unit cell materials and the designed porosities on the unit cell mechanical properties were given. The presented approach provides an effective tool for design and modeling complex bone tissue and for scaffold design. The calculated E from the characterization is in accordance with published data for cancellous bone in the range of 0.5-1.5GPa. It is important to note that both cancellous and cortical bone has been smeared together in our laminated composite model, and hence the slightly higher values of E obtained by our method. The curves presented in Figure 7 can aid in the selection of a unit cell with the required porosity and mechanical properties to match with that of the replaced bone. However, only one Young's modulus was calculated and used in this current study. The proposed process plan provides a road map on how an appropriate bone scaffold can be fabricated. The use of STEP to transfer the CAD model from the design software to the in house fabrication planning software entails advantages of transferring the complete product model data along with bone heterogeneity information in the future.

6. Acknowledgement

References

1. Langer, R and Vacanti, "Tissue Eningeering", Science 260, 920-026, 1993.
2. Langer, R., "Tissue Engineering: a new field and its challenges", *Sci Am.,* 280 (4), 86-9, 1999.
3. Nerem, R. M., Sambanis, A. "Tissue Engineering: from Biology to Biological Substitutes". *Tissue Engineering*, 1 (1), 1995.
4. Sun, W. and Lal, P., "Recent Development on Computer-Aided Tissue Engineering – A Review," *Journal of Computer Methods and Programs in Biomedicine,* Vol. 67 (2), pp. 85-103, 2002.
5. Lanza, R.P., Langer, R., and Chick, W.L., Principles of Tissue Engineering, Academic Press, 1997.
6. Marra, K., Campbell, P.G., DiMilla, P.A., Kumta, P., Mooney, M.P., Szem J., and Weiss, L., "Novel Three Dimensional Biodegradable Scaffolds for Bone Tissue Engineering", in Materials Research Society Fall Meeting, December, 1998.
7. Gomi K. and Davies, J.E., "Guided bone tissue elaborationby osteogenic cells in vitro," J. Biomed. Mater. Res. 4, 429-431, 1993.
8. Martin, R.B., "Determinants of Mechanical Properties of Bone", Biomechanics, 24, pp 79-88, 1991.
9. Hutmacher, D.W., "Scaffolds in tissue engineering bone and cartilage," Biomaterials, 21, pp. 2529-2543, 2000.

10. Hollister, S.J. Levy, R.A., Chu, T.W., Halloran, J.W., Feinberg, S.E., "An image based approach for designing and manufacturing craniofacial scaffolds", Int J of Oral and Maxillofacial surgery, 2000; 29; 67-71.
11. Starly, B., Lau, W., and Fang, Z., Sun, W. ""Biomimetic" Model for Heterogeneous Bone Scaffold", *Recent Development in Biomedical Engineering,* J Vossoughi (Editor), Medical and Engineering Publishers, 2002.
12. Sun, W., Darling, A., Subbaraman, G., "BioModeling Assisted Three-Dimensional Organ Printing", *Recent Development in Biomedical Engineering,* J Vossoughi (Editor), Medical and Engineering Publishers, 2002.
13. Sun, W., Starly, B., Lau, A., Lau, W. Lim, D., Seliktar, R., Youssef, A., Bradbury, T. and Gaylo, C., "Computer-Aided Design Modeling for Heterogeneous Bone Structure", *Proceedings of the American Society for Composites 17th Technical Conference*, Purdue University, 10/12-10/15, 2002.
14. MIMICS User Manual, Materialise, Leuven, Belgium, 2002.
15. GeoMagic User Manual, Raindrop Geomagic, Research Triangle, NC, USA, 2002.
16. Pro/Engineer User Manual, Parametric Technology Corporation, Wattham, MA, USA, 2002
17. Rice J.C, Cowin S.C, Bowman J.A, "On the dependence of elasticity and strength of cancellous bone on apparent density, J. Biomechanics, 21, 13-16. 1998
18. Rho, J.Y., Hobatho, M.C. and Ashman, R.B., "Relations of mechanical properties to density and CT numbers in human bone," Medical Engineering and Physics, 17, pp. 347-355, 1995.
19. Sun, W. and Hu, X., "Reasoning Boolean Operation Based CAD Modeling for Heterogeneous Objects," Journal of Computer Aided Design*, Vol. 34, pp. 481-488, 2002.
20. Sun, W., "Multi-volume CAD Modeling for Heterogeneous Object Design and Fabrication," Journal of Computer Science and Technology, Vol 15, No. 1, pp. 27 – 36, 2000
21. J. Owen, "STEP: a critical technology for business". Proceedings of the PDT Days 1993 Conference (49-92), ISBN 3-18-091096-8
22. J Owen, "STEP: An Introduction", 1997, Published by Information Geometers Ltd, UK, ISBN1-874728-11-9.
23. Dutta D, Kumar, V., Pratt, M. J., and Sriram R, "Towards STEP based Data Transfer in Layered Manufacturing", Proceedings of the 10th international conference IFIP, PROLOMAT Conference, Trento, Italy 1998.
24. Dutta, Debasish, "Adaptive Slicing of Hetergeneous Solid Models for Layered Manufacturing", Computers in Engineering Conference, DETC98/CIE-5698, – Atlanta, ASME
25. Patil. L., Dutta D, Pratt M.J., R.D. Sriram, "Representation of Heterogeneous Objects in ISO 10303 (STEP)", *Proceedings of the ASME Conference, Orlando, FL, November 5-11, 2000.*
26. Dolenc and I. Mäkelä, (1994) "Slicing procedures for layered manufacturing techniques," Computer-Aided Design, Vol. 26, No. 2, pp. 119-126.
27. Jamieson R. and Hacker H. (1995) "Direct Slicing of CAD Models for Rapid Prototyping", Rapid Prototyping Journal, Vol. 1 (2), pp. 4-12